Research Article

Absorbance Optical Properties Calculation of ABX_3 (A = Cs, Li; B = Pb; X = I, Br, Cl) Cubic Phase Using Density Functional Theory (DFT) Method

Aidha Ratna Fajarini Sidik[1], Pina Pitriana[2]*, and Hasniah Aliah[1]

[1]Physics Program Study, Faculty of Science and Technology, UIN Sunan Gunung Djati, Jl. A.H. Nasution, Bandung, Indonesia, 40614
[2]Physics Education Program Study, Faculty of Tarbiyah and Teacher Training, UIN Sunan Gunung Djati, Jl. A.H. Nasution, Bandung, Indonesia, 40614

ORCID
Pina Pitriana: https://orcid.org/0000-0001-6436-6309
Hasniah Aliah: https://orcid.org/0000-0002-4527-0253

Abstract.
Organic-inorganic perovskite is attracting much attention because it can be used for optoelectronic applications, such as solar cells and energy storage materials. In this study, we calculated the absorbance optical properties of perovskite ABX_3 (A = Cs, Li; B = Pb; X = I, Br, Cl) in the cubic phase using DFT, one of the most common methods for analyzing the optical properties of materials. These studies were undertaken to determine the optical absorbance properties of the ABX_3 perovskite as a potential for optoelectronic applications. The calculation was initiated by finding the optimization of pseudopotential and k_point, and pseudopotential GGA-PBE and k_point 8 x 8 x 8 are used as parameters to calculate absorbance optical properties. The absorbance calculation results are at a wavelength of 305.59 nm with a bandgap of 1.7608 eV for $CsPbBr_3$, 380.78 nm with a bandgap of 2.27 eV for $CsPbCl_3$, 301.86 nm with a bandgap of 1.35 eV for $CsPbI_3$, 225.04 nm with a bandgap of 1.72 eV for $LiPbBr_3$, 201.25 nm with a bandgap of 1.55 eV for $LiPbCl_3$, and 211.58 nm with a bandgap of 1.24 eV for LiPbI3. These results indicate that ABX_3 (A = Cs, Li; B = Pb; X = I, Br, Cl) has a good absorbance ability. These properties make ABX3 a potential material for optoelectronic applications.

Keywords: absorbance, optical properties, ABX_3, cubic phase, DFT

Corresponding Author: Pina Pitriana; email: pina.pitriana@uinsgd.ac.id

Published: 27 March 2024

Publishing services provided by Knowledge E

Selection and Peer-review under the responsibility of the ICMScE Conference Committee.

1. INTRODUCTION

Solar energy is one of Asia's most attractive renewable energy sources and is a significant energy source for global warming and the energy crisis. This energy can be harnessed through solar cells, which work by converting sunlight into electrical energy. The solar cell is a device with great potential to be developed. Solar cells have experienced significant developments, such as the emergence of silicon-based solar cells, thin-film solar cells to the third generation of solar cells, Dye-Sensitized Solar (DSSC) solar cells.

Compared to other solar cells, silicon-based solar cells, such as multijunction silicon solar cells and single crystal solar cells, have 46% and 25% efficiency [1]. However, these solar cells require complex fabrication and no small cost. Therefore, developing solar cells with easy fabrication at low cost is still a hot topic in research. Recently, perovskite solar cells have attracted attention because they have significant developments. These solar cells have achieved efficiencies of more than 20.1% [1].

Organic-inorganic perovskites are identified by the structural formula ABX_3, where A is an organic-inorganic ion, B is a divalent metal atom, and X is a halogen. These materials have attracted widespread interest due to their potential applications as solar cell absorbers [2], topological insulators [3], and even superconductors [4]. In 2018, perovskite-type methylammonium lead iodide ($MAPbI_3$) achieved a maximum light conversion efficiency of 23.7% [5]. However, the perovskite is chemically unstable due to the volatile and hygroscopic nature of the organic cations at high temperatures. Therefore, Perovskite Inorganic Metal Halide (IMH) emerged as a promising alternative with superior stability and comparable properties.

Quantum ESPRESSO (QE) is a tool used to calculate the electronic structure of a system or material model. The advantage of QE is that the base DFT cannot directly solve quantum mechanics, thus making calculations more effective. The analysis only includes the calculation of atomic shells to allow faster calculations [6].

Density Functional Theory (DFT) is one of the most commonly used methods for studying material properties in solid-state science. DFT was used to analyze perovskite materials' structure, electronic and optical properties [7]. Therefore, theoretical research on the electronic, structural, and optical properties of perovskite materials is essential to thoroughly understand this type of material. In this study, we will discuss the optical properties of the ABX_3 molecule, where A is an alkaline cation (A = Cs, Li), B is a divalent metal atom (B = Pb), and X is a halogen (X = I, Br, Cl) using the method DFT.

2. RESEARCH METHOD

In this research, the molecular structure used is the perovskite molecule ABX_3 (A = Cs, Li; B = Pb; X = I, Br, Cl) in the cubic phase with different lattice parameters in each molecule. This study carried out several optimizations, including inorganic iron halide molecules, namely $CsPbBr_3$, $CsPbCl_3$, $CsPbI_3$, $LiPbBr_3$ $LiPbCl_3$, $LiPbI_3$, optimization of Ecutwfc and Ecutrho, optimization of pseudopotential and optimization of K-Point.

The calculation stage is carried out after the molecular depiction using the VESTA software to obtain the atomic coordinates, which will be used in the next step. Input

files can be made using the Text Editor software. The data structures that need to be included in the input file include variables: system, control, electron, atomic species, atomic position, cell parameters, and K-point. Then the calculation phase of the input file is executed using the Quantum ESPRESSO software on kogence.com. The module used to calculate the total energy is plane waves (pw.x). After running the SCF calculation using the pw.x module to get the absorbance plot, it continued using the epsilon module (epsilon.x). The calculation results are then visualized using the OriginPro software. After all, stages have been carried out, the data obtained is analyzed and made into a report.

3. RESULTS AND DISCUSSION

3.1. Calculation Parameter Variation

TABLE 1: Total energy value (eV) with optimization of cut-off energy and K-points.

Molecule	Ecutwfc (Ry)	Ecutrho (Ry)	K-Point	Total Energy (Ry)
$CsPbBr_3$	30	240	6 x 6 x 6	-1900.13618367
			8 x 8 x 8	-1900.13649551
	60	480	6 x 6 x 6	-1900.13659316
			8 x 8 x 8	-1900.13667545
$CsPbCl_3$	30	240	6 x 6 x 6	-2846.47313233
			8 x 8 x 8	-2846.47324326
	60	480	6 x 6 x 6	-2846.47335463
			8 x 8 x 8	-2846.47347368
$CsPbI_3$	30	240	6 x 6 x 6	-2423.62794288
			8 x 8 x 8	-2423.62818986
	60	480	6 x 6 x 6	-2423.62826874
			8 x 8 x 8	-2423.62835480
$LiPbBr_3$	30	240	6 x 6 x 6	-2049.86768448
			8 x 8 x 8	-2049.87915466
	60	480	6 x 6 x 6	-2049.87925474
			8 x 8 x 8	-2049.87931137
$LiPbCl_3$	30	240	6 x 6 x 6	-1124.25740378
			8 x 8 x 8	-1124.25774124
	60	480	6 x 6 x 6	-1124.25788183
			8 x 8 x 8	-1124.25796745
$LiPbI_3$	30	240	6 x 6 x 6	-2022.77054174
			8 x 8 x 8	-2022.77098600
	60	480	6 x 6 x 6	-2022.77113448
			8 x 8 x 8	-2022.77256754

The initial calculation phase begins with the Self-Consistent Field (SCF), which will be used to calculate changes in the cut-off energy value and k-points. Each molecule's total energy (Ry) is obtained in calculating the parameter changes. K-points are also used to see the minimum total energy. The larger the k-points, the more time it takes to run the PWSCF calculation. The numerical results obtained indicate that the method can perform DFT calculations. DFT can be limited by calculating the value in SCF iterations. Accurate results can be obtained through consistent calculations. Table 1 describes the results of the parameters used in the calculations, namely the minimum total energy results with cut-off energy of 480 Ry and k-points 8×8×8. The minimum total energy of $CsPbBr_3$, $CsPbCl_3$, $CsPbI_3$, $LiPbBr_3$, $LiPbCl_3$, $LiPbI_3$ molecules is -1900.13667545 Ry, -2846.47347368 Ry, -2423.62835480 Ry, -2049.87931137 Ry, -1124.25796745 Ry, and -2022.77256754 Ry. Furthermore, these parameters are used to calculate the optical properties of the absorbance.

3.2. Absorbance Optical Properties

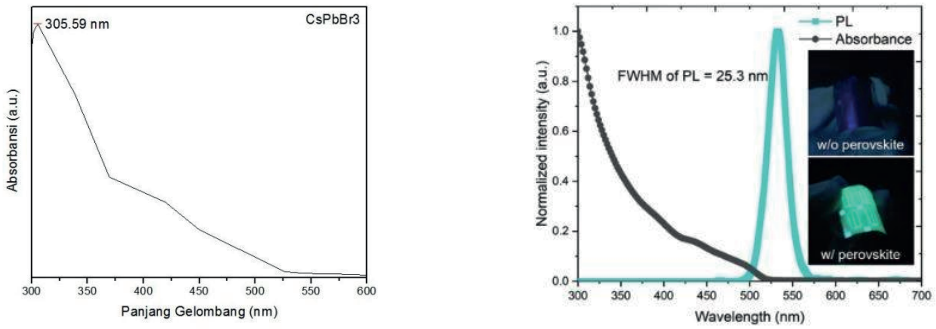

(a) (b)

Figure 1: (a) Absorbance spectrum of CsPbBr3. (b) Absorbance spectrum of CsPbBr3 [8].

$CsPbBr_3$ is an alkali metal halide perovskite material with semiconducting properties. In this study, the optical absorbance spectrum of the $CsPbBr_3$perovskite material is shown in Figure 1(a), the maximum absorbance was found at 305.59 nm. According to the experimental results Kim et al. in Figure 1(b), the $CsPbBr_3$ perovskite absorbs UV light from 300 to 520 nm with a maximum absorbance in the 300 nm wavelength range. Photons with a wavelength of 532 nm [8]. Figure 2 shows that this study resulted in a bandgap of 1.7608 eV for $CsPbBr_3$. The maximum absorbance and bandgap results indicate that $CsPbBr_3$ material is a promising semiconductor for solar cells.

In Figure 3(a), the maximum absorbance of the $CsPbCl_3$ molecule is at a wavelength of 380.78 nm. According to the research results Pandey, Kumar and Chakrabarti in Figure 3(b), the maximum absorbance of the $CsPbCl_3$ molecule is 398 nm [9]. While

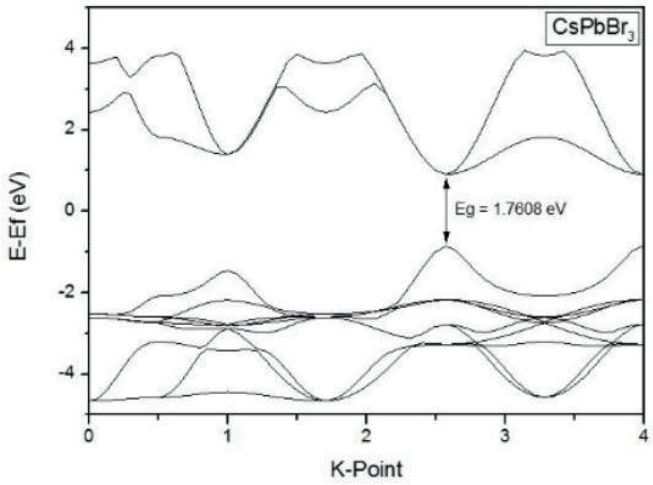

Figure 2: Bandgap curve of CsPbBr3.

the study results Szeremeta et al. for the $CsPbCl_3$ molecule, the maximum absorbance was 409 nm [10]. While in Figure 4, this study produces a bandgap of 2.27 eV for $CsPbCl_3$. Overall, $CsPbCl_3$ has attractive properties required for various optoelectronic and photovoltaic devices.

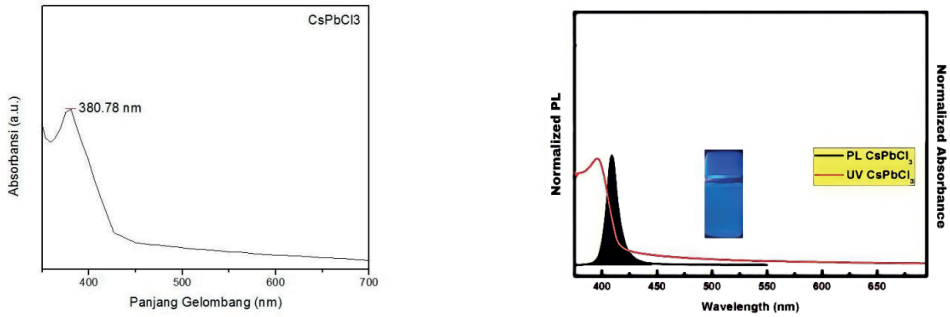

(a) (b)

Figure 3: (a) Absorbance spectrum of $CsPbCl_3$. (b) Absorbance spectrum of $CsPbCl_3$ [9].

The absorbance spectrum of the $CsPbI_3$ molecule in Figure 5(a) has a maximum absorbance of 301.86 nm. According to the calculation results Jing, Sa and Xu in Figure 5(b), $CsPbI_3$ shows stronger optical absorption in the visible light region between 300 and 400 nm with a maximum absorbance of 305 nm [11]. $CsPbI_3$ has a suitable bandgap (1.34 eV). In addition, the narrowing of the bandgap indicates an increase in optical absorption in the visible light region in Figure 6 with a bandgap of 1.35 eV, which may have great potential for optoelectronic devices.

Figure 7(a) shows that the absorbance spectrum of $LiPbBr_3$ has an absorbance range of 225 – 600 nm with a maximum absorbance of 225.04 nm. Figure 7(b) shows that the absorbance spectrum of $LiPbCl_3$ has an absorbance range of 200 – 500 nm with a

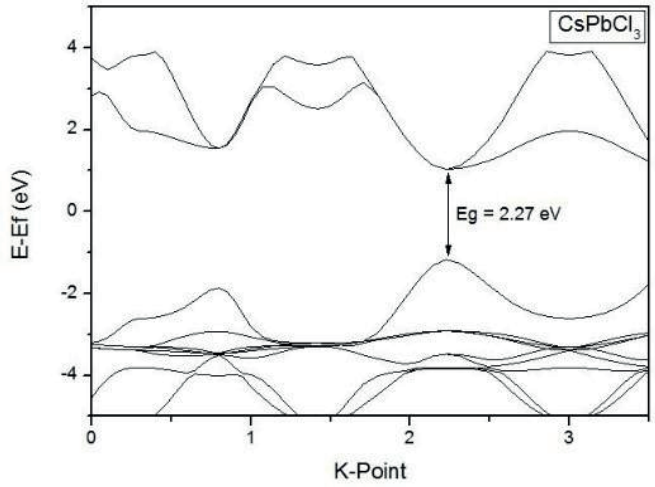

Figure 4: Bandgap curve of $CsPbCl_3$.

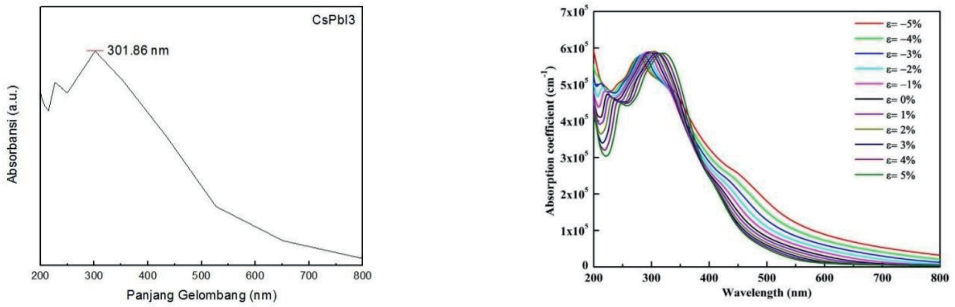

(a) (b)

Figure 5: (a) Absorbance spectrum of CsPbI3. (b) Absorbance spectrum of CsPbI3 [11].

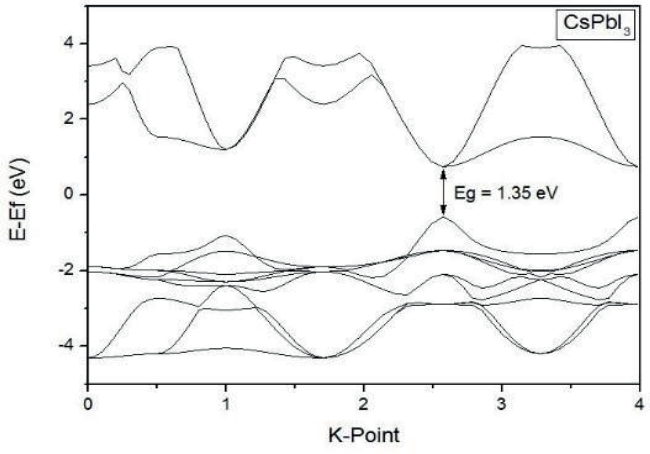

Figure 6: Bandgap curve of $CsPbI_3$.

maximum absorbance of 201.25 nm. Moreover, Figure 7(c) shows that the absorbance spectrum of $LiPbI_3$ has an absorbance range of 205 – 800 nm with a maximum absorbance of 211.58 nm.

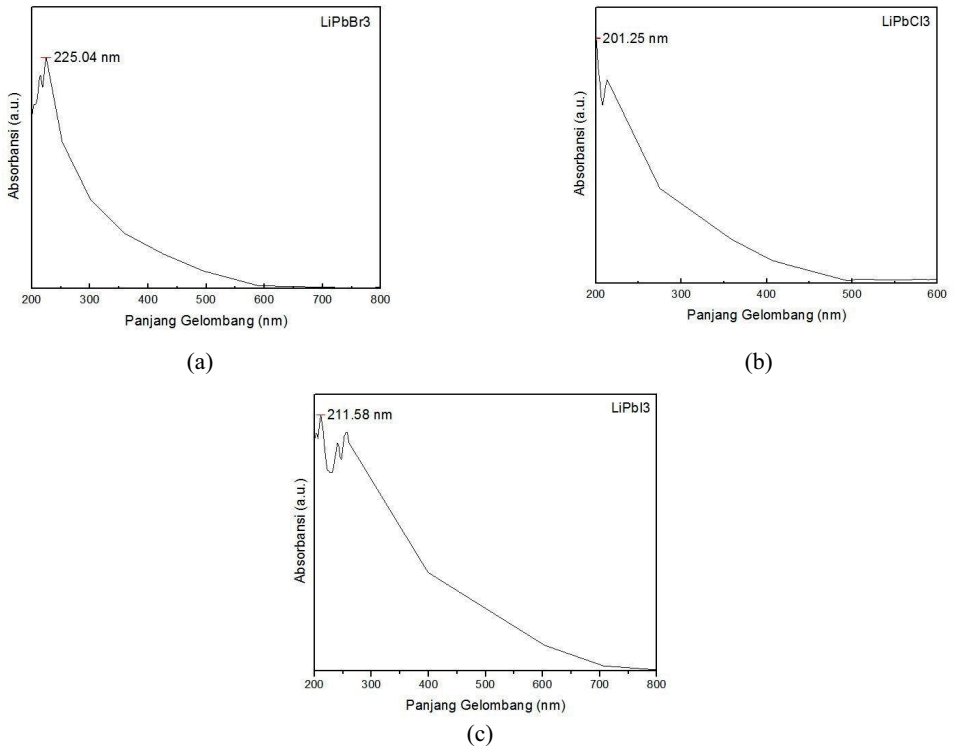

Figure 7: (a) Absorbance spectrum of $LiPbBr_3$. (b) Absorbance spectrum of $LiPbCl_3$. (c) Absorbance spectrum of $LiPbI_3$.

Belabbas et al. analyzed the stability of the compound $LiPb(Br:Cl:I)_3$ to achieve electronic properties and improve photocatalytic performance under visible light. $LiPb(Br:Cl:I)_3$ showed a bandgap of (2.01; 2.87 and 1.40) eV [12]. Meanwhile, according to the calculation results of the bandgap curve in Figure 8(a), the bandgap of $LiPbBr_3$ is 1.72 eV. In Figure 8(b), the bandgap of $LiPbCl_3$ is 1.55 eV and the bandgap of LiPbI3 is 1.24 eV in Figure 8(c). These results indicate that the $LiPb(Br:Cl:I)_3$ material is suitable for maximizing the absorbance spectrum, and $LiPbI_3$ has a higher absorbance coefficient in the visible range.

4. CONCLUSION

In this study, a known peak value can determine the wavelength of light absorbed by the molecule. Maximum wavelength means the molecule can absorb maximum light at that peak wavelength. The ABX_3 (A = Cs, Li; B = Pb; X = I, Br, Cl) molecules can broaden the absorption spectrum of photons of sunlight and convert them into electrical energy. The absorbance value decreases along with the higher absorption wavelength.

The efficiency of a solar cell material varies with its bandgap, while the bandgap depends on different physical parameters and phase transitions. To understand the

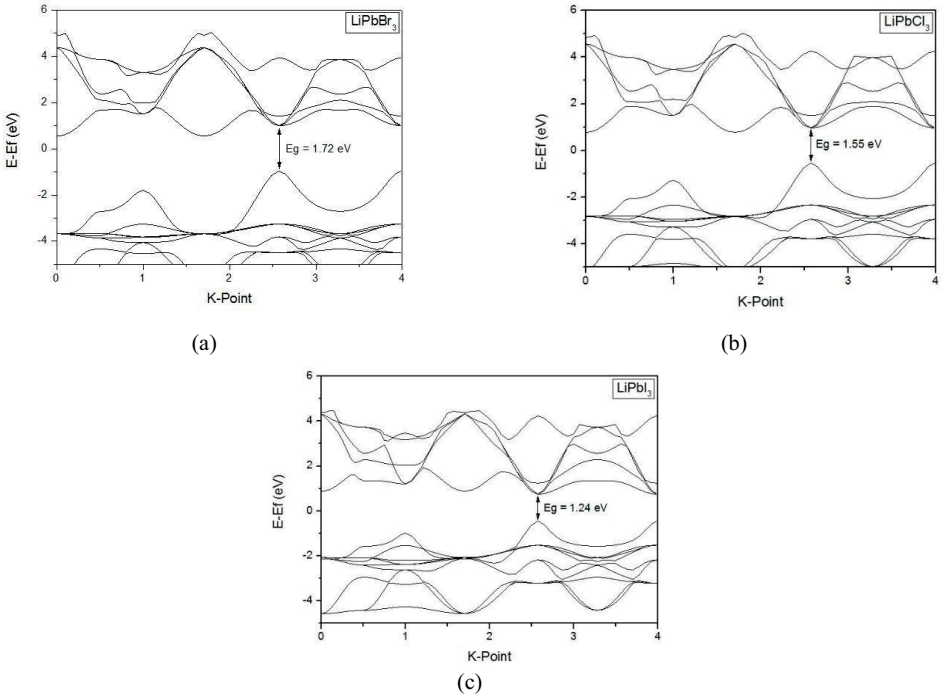

Figure 8: (a) Bandgap curve of $LiPbBr_3$. (b) Bandgap curve of $LiPbCl_3$. (c) Bandgap curve of $LiPbI_3$.

efficiency of solar cells, complete knowledge of the parameters affecting the bandgap and all the compound phases is necessary. For mechanical properties, the values obtained indicate that the ABX_3 molecule (A = Cs, Li; B = Pb; X = I, Br, Cl) is mechanically and dynamically stable [13]. Band structure analysis shows that all molecules have semiconductor behavior for electronic properties. The absorbance spectrum above indicates that all compounds are promising semiconductors for optoelectronic applications. However, it can be seen from the maximum absorbance spectrum that $CsPbX_3$ (X= I, Br,Cl) has a more significant potential than $LiPbX_3$ (X= I, Br,Cl).

References

[1] Ch P, Pbi NH, Saraswati EM, Addini D, Permatasari FA, Aimon AH. Studi awal impedansi elektrokimia lapisan tipis. 2015. pp. 124–8.

[2] Lang L, Yang JH, Liu HR, Xiang HJ, Gong XG. First-principles study on the electronic and optical properties of cubic ABX3 halide perovskites. Phys Lett A. 2014;378(3):290–3.

[3] Jin H, Im J, Freeman AJ. Topological insulator phase in halide perovskite structures. Phys Rev B Condens Matter Mater Phys. 2012;86(12):121102.

[4] Takahashi Y, Obara R, Lin ZZ, Takahashi Y, Naito T, Inabe T, et al. Charge-transport in tin-iodide perovskite CH3NH3SnI3: origin of high conductivity. Dalton Trans. 2011 May;40(20):5563–8.

[5] A. Swarnkar, A.R. Marshall, E.M. Sanehira, et al., "Quantum dot–induced phasestabilization of a-CsPbI3perovskitefor high-efficiency photovoltaics.," *Science*. vol. 354, no. 6308, pp. 92 LP—- 95, 2016.

[6] Barnes TA, Kurth T, Carrier P, Wichmann N, Prendergast D, Kent PR, et al. Improved treatment of exact exchange in quantum ESPRESSO. Comput Phys Commun. 2017;214:52–8.

[7] Afsari M, Boochani A, Shirdel F. Electronic and optical properties of two propounded compound in photovoltaic applications, $CsPbI_3$ and $CH_3NH_3PbI_3$: by DFT. Optik (Stuttg). 2019;199:163360.

[8] Kim YC, Jeong HJ, Kim ST, Song YH, Kim BY, Kim JP, et al. Luminescent down-shifting $CsPbBr_3$ perovskite nanocrystals for flexible $Cu(In,Ga)Se_2$ solar cells. Nanoscale. 2020 Jan;12(2):558–62.

[9] Pandey N, Kumar A, Chakrabarti S. Investigation of the structural, electronic, and optical properties of Mn-doped $CsPbCl_3$: theory and experiment. RSC Adv. 2019 Sep;9(51):29556–65.

[10] Szeremeta J, Antoniak MA, Wawrzyńczyk D, Nyk M, Samoć M. The two-photon absorption cross-section studies of $CsPbX_3$ (X = I, Br, Cl) nanocrystals. Nanomaterials (Basel). 2020 May;10(6):1–12.

[11] Jing H, Sa R, Xu G. Tuning electronic and optical properties of CsPbI3 by applying strain: A first-principles theoretical study. Chem Phys Lett. 2019;732(July):4–7.

[12] Belabbas M, Marbouh N, Arbouche O, Hussain A. Optoelectronic properties of the novel perovskite materials LiPb(Cl:Br:I)3 for enhanced hydrogen production by visible photo-catalytic activity: Theoretical prediction based on empirical formulae and DFT. Int J Hydrogen Energy. 2020;45(58):33466–77.

[13] Bourachid I, Caid M, Cheref O, Rached D, Heireche H, Abidri B, et al. Insight into the structural, electronic, mechanical and optical properties of inorganic lead bromide perovskite $APbBr_3$ (A = Li, Na, K, Rb, and Cs). Computational Condensed Matter. 2020;24:e00478.